Cholesterol depletion enhances TGF-β Smad signaling by increasing c-Jun expression through a PKR-dependent mechanism

Keren E. Shapira[a], Marcelo Ehrlich[b],*, and Yoav I. Henis[a],*
[a]Department of Neurobiology and [b]Department of Cell Research and Immunology, George S. Wise Faculty of Life Sciences, Tel Aviv University, Tel Aviv 69978, Israel

ABSTRACT Transforming growth factor-β (TGF-β) plays critical roles in numerous physiological and pathological responses. Cholesterol, a major plasma membrane component, can have pronounced effects on signaling responses. Cells continually monitor cholesterol content and activate multilayered transcriptional and translational signaling programs, following perturbations to cholesterol homeostasis (e.g., statins, the commonly used cholesterol-reducing drugs). However, the cross-talk of such programs with ligand-induced signaling responses (e.g., TGF-β signaling) remained unknown. Here, we studied the effects of a mild reduction in free (membrane-associated) cholesterol on distinct components of TGF-β–signaling pathways. Our findings reveal a new regulatory mechanism that enhances TGF-β–signaling responses by acting downstream from receptor activation. Reduced cholesterol results in PKR-dependent eIF2α phosphorylation, which enhances c-Jun translation, leading in turn to higher levels of JNK-mediated c-Jun phosphorylation. Activated c-Jun enhances transcription and expression of Smad2/3. This leads to enhanced sensitivity to TGF-β stimulation, due to increased Smad2/3 expression and phosphorylation. The phospho/total Smad2/3 ratio remains unchanged, indicating that the effect is not due to altered receptor activity. We propose that cholesterol depletion induces overactivation of PKR, JNK, and TGF-β signaling, which together may contribute to the side effects of statins in diverse disease settings.

INTRODUCTION

Transforming growth factor-β (TGF-β) ligands mediate multiple physiological and pathological responses, including metabolic regulation, inflammation, and cancer (Markowitz *et al.*, 1995; Roberts and Wakefield, 2003; Sanjabi *et al.*, 2009; Gatza *et al.*, 2010; Heldin

et al., 2012; Massague, 2012; Tan *et al.*, 2012; Meng *et al.*, 2016). TGF-β signals via two dual-specificity (Ser/Thr and Tyr) kinase receptors, type I (TβRI) and type II (TβRII; Shi and Massague, 2003; Gordon and Blobe, 2008; Heldin and Moustakas, 2016). It binds to TβRII, which then recruits and phosphorylates TβRI. In turn, TβRI phosphorylates Smad2/3 proteins, mediating their translocation together with Smad4 to the nucleus, where they regulate transcription of target genes (Shi and Massague, 2003; Moustakas and Heldin, 2009; Budi *et al.*, 2017). TGF-β can also signal via non-Smad pathways, including c-Jun N-terminal kinase (JNK; Hanafusa *et al.*, 1999; Hocevar *et al.*, 1999; Bakin *et al.*, 2000; Galliher and Schiemann, 2007; Sorrentino *et al.*, 2008; Yamashita *et al.*, 2008). TGF-β signaling is regulated at multiple levels. At the receptor level, regulation may take place by interactions between the signaling receptors (reviewed in Ehrlich *et al.*, 2012), through their domain distribution at the plasma membrane (Shapira *et al.*, 2014; Budi *et al.*, 2015), endocytosis/recycling (Lu *et al.*, 2002; Penheiter *et al.*, 2002; Di Guglielmo *et al.*, 2003; Chen *et al.*, 2009; Shapira *et al.*, 2012), and their synthesis or degradation (Massague and Wotton, 2000; Shi and Massague, 2003; Amsalem *et al.*, 2016). At the level of downstream

signaling by Smads, signaling is tuned by a number of posttranslational modifications, which affect the composition of Smad complexes, their activation, intracellular localization, and degradation (Wrighton and Feng, 2008; Hill, 2009; Xu et al., 2012).

All these processes may be modulated by cholesterol, a plasma membrane organizer whose levels determine the formation of cholesterol/sphingolipid-enriched domains termed lipid rafts (Simons and Toomre, 2000; Hancock, 2006; Jacobson et al., 2007; Eisenberg et al., 2011; Parton and del Pozo, 2013). Cholesterol homeostasis is tightly regulated by mechanisms controlling sterol synthesis, uptake, and turnover (Goedeke and Fernandez-Hernando, 2012; Luu et al., 2013). These processes respond to alterations in cellular context (e.g., cell stress [Werstuck et al., 2001]) and to signaling pathways such as mitogen-activated protein kinase, phosphatidylinositol-3-kinase (PI3K), AMP-activated protein kinase, and more (Motoshima et al., 2006; Gorin et al., 2012). Conversely, changes in the cellular cholesterol level (e.g., due to statin-mediated inhibition of HMG-CoA reductase) evoke multilayered cellular responses aimed at restoring cholesterol homeostasis (Gabitova et al., 2014).

The effects of cholesterol depletion on TGF-β signaling are still under debate (Razani et al., 2001; Di Guglielmo et al., 2003; Zuo and Chen, 2009; Shapira et al., 2014; Muthusamy et al., 2015), and the potential effects of cholesterol on downstream TGF-β signaling components (as opposed to effects at the level of the receptors) have not been thoroughly investigated. The potential regulation of TGF-β signaling downstream components by cholesterol has important implications in view of the use of statins, which are metabolic inhibitors of cholesterol production, in a broad spectrum of therapy settings, conditions that can alter TGF-β signaling and its physiological outcomes. In the current work, we investigated the effects of mild cholesterol depletion (30% reduction in free cholesterol) on TGF-β signaling. We employed Mv1Lu mink lung epithelial cells, which are highly responsive to TGF-β and were broadly employed in studies on TGF-β signaling, as well as MLE 12 mouse lung epithelial cells. Our results reveal a new mechanism by which reduced cholesterol enhances TGF-β signaling downstream from the receptors. Such a reduction induces overactivation of double-stranded RNA-dependent protein kinase (PKR) and JNK, resulting in enhanced translation and activation of c-Jun. In turn, this elevates Smad2/3 transcription and expression, resulting in augmented TGF-β–induced Smad3-mediated responses.

RESULTS

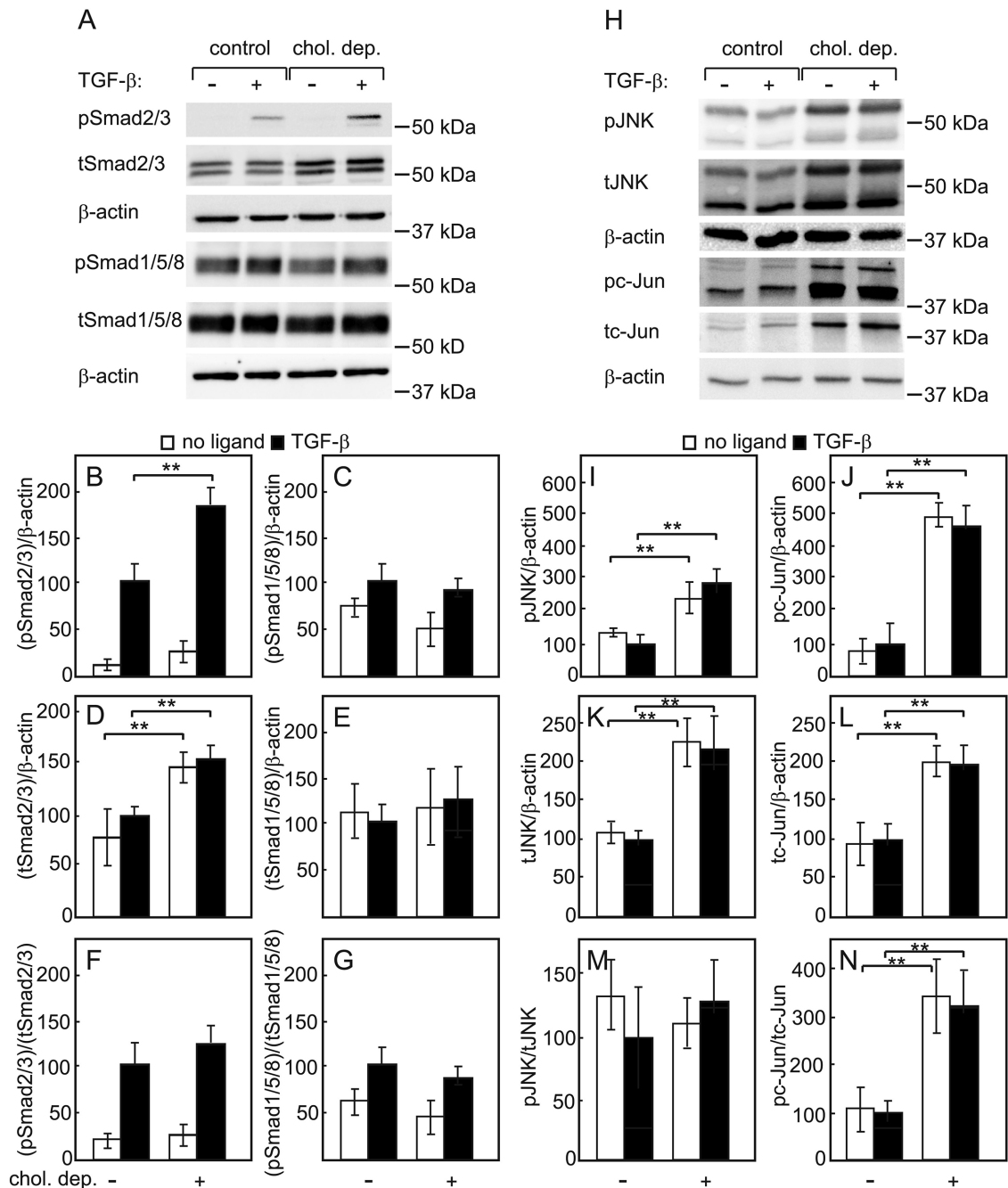### Statin-mediated cholesterol depletion enhances Smad2/3 and JNK/c-Jun TGF-β signaling pathways

In spite of the potential involvement of cholesterol-dependent lipid rafts in TGF-β signaling (Razani et al., 2001; Di Guglielmo et al., 2003; Zuo and Chen, 2009; Shapira et al., 2014; Muthusamy et al., 2015), the effects of cholesterol on downstream TGF-β signaling components are not known. Because the most common cholesterol-reducing treatment is by statins, such effects are of high relevance to TGF-β–related cancers and other diseases, as the cholesterol depletion treatment alters the cellular context, potentially changing the response to TGF-β signaling. We set to explore the potential effects of reducing the membrane cholesterol content on downstream TGF-β signaling pathways in Mv1Lu mink lung epithelial cells, which are highly responsive to TGF-β, and provided the basis for the widely accepted features of TGF-β signaling (Laiho et al., 1990; Wrana et al., 1992). The free cholesterol level in Mv1Lu cells was reduced by treatment with lovastatin (50 μM) in the presence of 50 μM mevalonate (see Materials and Methods), or (in control experiments) by cholesterol absorption with 2-hydroxypropyl-β-cyclodex-trin (HPβCD). While the statin inhibits HMG-CoA reductase, the product of this enzyme (mevalonate) is added at a concentration low enough to reduce cholesterol synthesis but sufficient to maintain prenylation and geranylgeranylation (Eisenberg et al., 2006, 2011; Shvartsman et al., 2006). The conditions employed resulted in mild and similar reduction in the total free (nonesterified) cholesterol content (~30%; Supplemental Figure S1). The lovastatin-mediated cholesterol depletion elevated both total Smad2/3 and the TGF-β–stimulated formation of pSmad2/3, with no effects on the BMP-related Smads (Smad1/5/8; Figure 1, A–G). The increase in total (tSmad2/3) and pSmad2/3 was by a similar factor, leaving the ratio between them unaltered (Figure 1F). It should be noted that the lack of change in the phospho/total Smad2/3 ratio indicates that the increase in pSmad2/3 is not a result of augmented receptor activity, but rather reflects the elevated levels of tSmad2/3. While tSmad2/3 appeared as two bands, the anti-pSmad2/3 antibody labeled a single band. Because this could reflect different affinities of the anti-pSmad2/3 antibody to pSmad2 versus pSmad3, we employed specific anti-Smad2, anti-Smad3, anti-pSmad2, or anti-pSmad3 antibodies (Supplemental Figure S2). These experiments showed that the total protein levels and the phosphorylation of Smad2 and Smad3 following TGF-β stimulation are both elevated by cholesterol depletion. The total JNK (tJNK), phospho-JNK (pJNK), total c-Jun (tc-Jun), and phospho c-Jun (pc-Jun) were also elevated. However, the effect on these major constituents of the JNK/c-Jun non-Smad pathway was constitutive (independent of TGF-β stimulation; Figure 1, H–N), further supporting the notion that the cholesterol depletion enhancement of downstream TGF-β signaling components does not depend on enhanced receptor activity. The concomitant increase in these two components is in line with c-Jun being a phosphorylation target of JNK, and with the ability of c-Jun to regulate its own transcription as well as that of JNK (Angel et al., 1988; Ventura et al., 2003). Control experiments (Supplemental Figure S3, A–G) show that incubation with lipoprotein-deficient serum (LPDS) alone (without statin) has no significant effects. Of note, the effects of cholesterol depletion on the expression and activation of TGF-β signal mediators are not restricted to Mv1Lu cells; essentially identical results were obtained using MLE 12 mouse lung epithelial cells (Supplemental Figure S4).

To validate that the effects measured are due to cholesterol depletion and not the result of potential other effects of statin treatment, we conducted control experiments where the cholesterol level was reduced to a similar degree by cholesterol absorption using a β-cyclodextrin derivative that binds and sequesters cholesterol in its hydrophobic core; we employed HPβCD, which is more selective for cholesterol than methyl-β-cyclodextrin (Christian et al., 1997) and is used for treatment of Nieman-Pick disease (Rosenbaum and Maxfield, 2011) and potentially additional diseases (Zimmer et al., 2016). The results (Figure 2, A–G) were similar to those obtained with the statin treatment, demonstrating that the effects are due to lower cholesterol levels.

The initial cellular response to TGF-β–mediated Smad2/3 stimulation is transcriptional regulation of target genes. To test whether the effects of cholesterol depletion on the pSmad2 and/or pSmad3 levels are translated to transcriptional responses, we conducted transcriptional activation assays (as described by us earlier; Shapira et al., 2012) comparing untreated and statin-treated cells. We employed several Smad-responsive luciferase reporter constructs. p3TP-Luc(+) (Wrana et al., 1992) and (CAGA)$_{12}$-Luc (Dennler et al., 1998; Shapira et al., 2012), which are mainly responsive to pSmad3, showed elevated transcriptional activation in response to TGF-β in cholesterol-depleted cells (Figure 3, A and B). Interestingly,

FIGURE 1: Cholesterol depletion has distinct effects on Smad2/3 and JNK/c-Jun levels and phosphorylation. Mv1Lu cells grown in 35-mm dishes were subjected (or not) to statin-mediated cholesterol depletion as described in *Materials and Methods*. After 16 h, they were serum-starved (2 h), incubated with or without 50 pM TGF-β1 (30 min), lysed, and analyzed by immunoblotting for total (t) and phosphorylated (p) Smad2/3, Smad1/5/8, JNK, and c-Jun. β-actin served as loading control. The bands were quantified by ECL (see *Materials and Methods*). (A) A representative blot (one out of six independent experiments in each case) of Smad2/3 and Smad1/5/8. (B–G) Quantification of total and phosphorylated Smad2/3 (B, D, F) and Smad1/5/8 (C, E, G) in untreated (control) and cholesterol-depleted cells. The untreated control sample with TGF-β1 was defined as 100%. Both tSmad2/3 and pSmad2/3 levels are elevated by a similar factor upon cholesterol depletion, such that the ratio between them is retained. No significant effects were detected in tSmad1/5/8 or pSmad1/5/8 following cholesterol depletion. (H) A representative blot of JNK and c-Jun immunoblots. (I–N) Quantification of total and phosphorylated JNK (I, K, M) and c-Jun (J, L, N) in untreated and in cholesterol-depleted cells. The untreated sample with TGF-β1 was taken as 100%. Both tJNK, pJNK and tc-Jun, pc-Jun levels increase following cholesterol depletion; however, this response is insensitive to TGF-β1. While the pJNK/tJNK ratio is unaltered, that of pc-Jun/tc-Jun is elevated following cholesterol depletion (panels M, N), reflecting the higher phosphorylation of c-Jun under these conditions, in line with its role as a phosphorylation target for JNK. Each bar is the mean ± SEM of six independent experiments (**, $P < 0.01$; Student's two-tailed t test). Control experiments (Supplemental Figure S3, A–G) show that incubation with LPDS alone (without statin) has no significant effects.
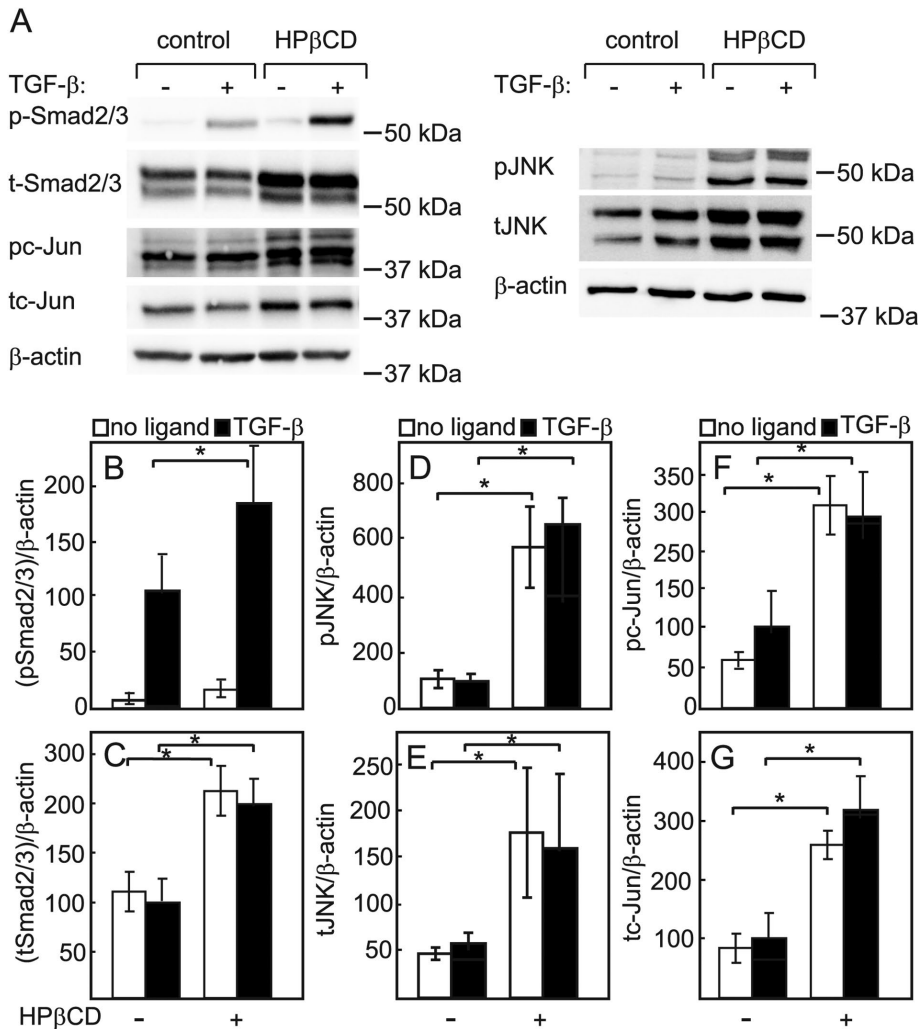
FIGURE 2: Cholesterol absorption with HPβCD affects Smad2/3 and JNK/c-Jun levels and phosphorylation similar to statin treatment. Cells were treated with HPβCD (16 h, similar to the statin treatment) to reduce their membrane cholesterol content (*Materials and Methods*). They were then treated with TGF-β1 and subjected to immunoblotting as in Figure 1. (A) A representative blot (one out of five independent experiments) of pSmad2/3, tSmad2/3, pJNK, tJNK, pc-Jun, and tc-Jun. β-Actin served as a loading control. (B–G) Quantification of total and phosphorylated proteins. In each panel, the untreated control sample with TGF-β1 was taken as 100%. (B) pSmad2/3. (C) tSmad2/3. (D) pJNK. (E) tJNK. (F) pc-Jun. (G) tc-Jun. The results resembled those obtained following cholesterol depletion by statin treatment (Figure 1), with reduced cholesterol inducing a similar increase in tSmad2/3 and pSmad2/3, enhancing also the formation of pSmad2/3 in response to TGF-β1. The levels of tJNK, pJNK, tc-Jun, and pc-Jun were also elevated, a response which was not altered by TGF-β1. Each bar is the mean ± SEM of five independent experiments (*, $P < 0.05$; Student's two-tailed t test).

TGF-β1 to induce loss of E-cadherin and increase in Snail; alteration of expression of these markers is a hallmark of EMT. Cholesterol depletion increased the level of E-cadherin in Mv1Lu cells, but made the loss of E-cadherin following TGF-β1 stimulation even more pronounced (Figure 4, A and B). Concomitantly, cholesterol depletion elevated the TGF-β-induced increase in Snail (Figure 4, A and C). Because EMT usually leads to enhanced cell migration, we studied the effects of cholesterol depletion on the migration of Mv1Lu cells in wound healing scratch assays (Figure 4, D–F). As expected, wound healing in Mv1Lu cultures was stimulated by TGF-β1. Cholesterol depletion by itself inhibited Mv1Lu wound healing, in line with the elevated level of E-cadherin under such conditions (Figure 4, A and B). This effect was significantly reduced by TGF-β, in line with the elevated level of pSmad2/3 (Figure 1), the reduced level of E-cadherin, and the enhanced expression of Snail (Figure 4).

Cholesterol depletion enhances Smad2/3 transcription and c-Jun translation

After establishing that cholesterol depletion increases the levels of total and phosphorylated Smad2/3 and c-Jun and affects their biological signaling, we investigated the mechanism(s) underlying these phenomena. Elevated expression levels of specific proteins, such as Smad2/3 and c-Jun, may stem from slower degradation rates or from increased synthesis (enhanced transcription and/or translation). To explore the contribution of the former mechanism, we compared Smad2/3 and c-Jun degradation rates in untreated or cholesterol-depleted Mv1Lu cells, in the presence of cycloheximide (CHX). Smad2/3 degradation was very slow and was unaffected by cholesterol depletion (Supplemental Figure S5, A and B). c-Jun degraded faster (7–8%/h), and was also unaffected by the same treatment (Supplemental Figure S5, D and E). Similar results were obtained in the presence of TGF-β (100 pM; Supplemental Figure S5, C and F). We conclude that altered degradation does not contribute significantly to the higher Smad2/3 or c-Jun levels in cholesterol-depleted cells.

To test whether the enhanced levels of Smad2/3 and c-Jun following cholesterol depletion are due to effects on their transcription (resulting in higher mRNA levels, and thus higher expression), we employed the general transcription inhibitor, actinomycin D. Treatment with actinomycin D blocked the effects of statin-mediated cholesterol depletion on Smad2/3 and c-Jun protein levels, including the TGF-β–mediated increase in pSmad2/3 (Figure 5, A–E). Because inhibition of transcription would also inhibit the ensuing translation, we proceeded to study the effects of cholesterol depletion on the mRNA levels of Smad2, Smad3, and c-Jun

pAR3-Lux (Hayashi *et al.*, 1997), which is responsive to pSmad2, was activated by TGF-β in the presence of Fast-1, but this response was insensitive to cholesterol depletion (Figure 3C). Thus, it appears that although both Smad3 and Smad2 are phosphorylated and their levels increase following cholesterol depletion, the downstream responses are mediated mainly by pSmad3. pBRE-Luc (Korchynskyi and ten Dijke, 2002), which is responsive to pSmad1/5/8, was not activated by TGF-β (Figure 3D), in line with the lack of phosphorylation of Smad1/5/8 under these conditions (Figure 1).
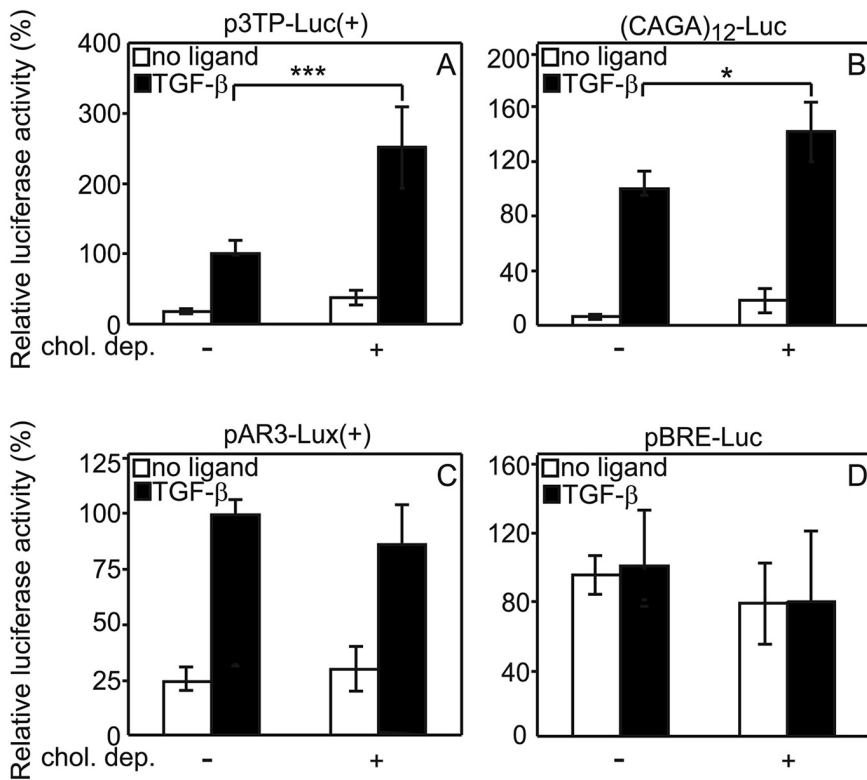
One of the established cellular responses of epithelial cells to TGF-β is epithelial-to-mesenchymal transformation (EMT; Bhowmick *et al.*, 2001; Moustakas and Heldin, 2016). We therefore examined the effect of statin-mediated cholesterol depletion on the ability of

FIGURE 3: Cholesterol depletion elevates Smad3-dependent TGF-β–mediated transcriptional activation. Mv1Lu cells were cotransfected with a TGF-β–superfamily responsive luciferase reporter plasmid: p3TP-Luc(+) (A), $(CAGA)_{12}$-Luc (B), pAR3-Lux with CMV-Fast1 (C), or pBRE-Luc (D), together with pRL-TK. At 12 h posttransfection, cells were subjected (or not; control) to statin-mediated cholesterol depletion as in Figure 1, serum-starved, stimulated (or not) with TGF-β1, and analyzed by the DLR assay. The results were normalized for transfection efficiency using Renilla luminescence. Data are presented as the percentage of activation relative to untreated cells stimulated with TGF-β1, taken as 100%. Each bar is the mean ± SEM of five independent experiments (***, $P < 0.01$; *, $P < 0.05$; Student's two-tailed t test).

(Figure 5, F–H). These studies showed that cholesterol depletion results in elevated mRNA levels of Smad2 and Smad3, but not of c-Jun. Such elevated mRNA levels may reflect either slower mRNA degradation or increased transcription. Therefore, we blocked transcription with actinomycin D and measured the transcript levels of Smad2, 3, and c-Jun over time by real-time reverse transcriptase-PCR (RT-PCR). Cholesterol depletion did not stabilize any of these mRNAs, ruling out mRNA stabilization as a potential mechanism (Figure 5, I–K). Taken together, these experiments suggest that the effects of cholesterol depletion on Smad2/3 levels are mediated via transcriptional regulation, while those on c-Jun occur at a later step (e.g., translation). To explore this issue, we measured the synthesis levels of the above proteins by $[^{35}S]$(Met+Cys) incorporation. As expected based on the enhanced transcription of Smad 2 and 3, Smad2/3 synthesis was elevated following cholesterol depletion (Figure 6, A and B). The level of c-Jun synthesis was increased even to a higher extent, in spite of the insensitivity of its transcription to cholesterol depletion (Figure 6, C and D). It follows that the enhanced expression of c-Jun mediated by cholesterol depletion involves effects on its translation.

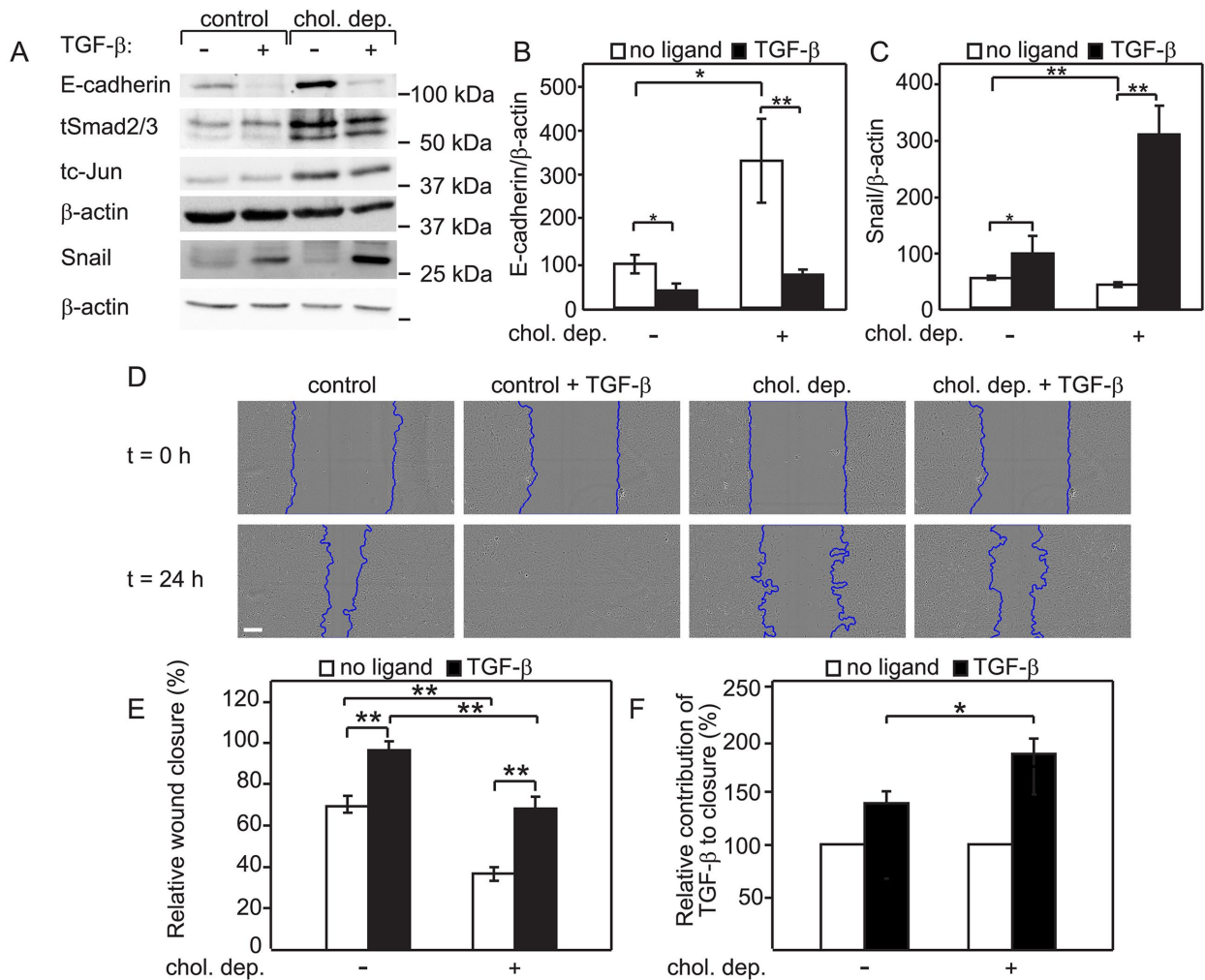## The effects of cholesterol depletion on c-Jun precede those on Smad2/3 and require PKR activity

c-Jun is involved in the transcriptional regulation of Smads and AP-1 (Liberati et al., 1999; Wong et al., 1999). We therefore investigated

whether activation of the JNK/c-Jun pathway is upstream to the effects of cholesterol depletion on Smad2/3. Figure 7, A–C, shows that the JNK inhibitor SP600125 inhibited formation of pc-Jun as expected. This resulted in prevention of both the elevation in tSmad2/3 and in TGF-β–mediated pSmad2/3 by cholesterol depletion. The requirement for c-Jun activation is supported by the finding that TGF-β1–induced transcriptional activation of the Smad pathway transcriptional reporters p3TP-Luc(+) and $(CAGA)_{12}$-Luc, which was enhanced by cholesterol depletion, was disrupted by the inhibitor (Figure 7, D and E). We conclude that the cholesterol depletion effect on JNK/c-Jun precedes that on Smad2/3, a conclusion supported by the finding (Supplemental Figure S6, A–C) that the TβRI (ALK5) inhibitor SB431542, which blocks Smad2/3 phosphorylation, does not inhibit the elevation in c-Jun levels and/or the ensuing increase in tSmad2/3. In addition, we tested the effects of the JNK inhibitor on the EMT markers (Supplemental Figure S7). In accord with the notion that JNK is required for the downstream effects of cholesterol on TGF-β signaling, the effects of cholesterol depletion on both E-cadherin and Snail were disrupted. It should be noted that SP600125 also inhibited the EMT response to TGF-β in untreated cells, in line with the involvement of JNK and c-Jun in EMT.

Multiple lines of evidence support the regulation of c-Jun expression at the level of translation (Sehgal et al., 2000; Polak et al., 2006; Spruill and McDermott, 2009). Specifically, sequence elements in the 5' untranslated region of c-Jun mRNA are thought to drive cap-independent translation in correlation with the phosphorylation of the eukaryotic initiation factor 2α (eIF2α), a common occurrence in cell stress. We therefore tested the effects of cholesterol depletion (with or without TGF-β) on eIF2α phosphorylation. This treatment led to a significant increase in eIF2α phosphorylation, an effect that was independent of TGF-β stimulation (Figure 8, A and B). Both effects are correlated with the increased expression of c-Jun (Figure 1H and Figure 6, C and D) and its independence of TGF-β stimulation (Figure 1).

A main regulator of eIF2α phosphorylation is PKR, the interferon-induced, double-stranded RNA-activated protein kinase (encoded by the EIF2AK2 gene). To test for the involvement of PKR in the effects described above, we employed the specific PKR inhibitor C16. In line with a role for PKR in the induction of eIF2α phosphorylation by cholesterol depletion, C16 abrogated the effect (Figure 9A). Accordingly, no increase in tc-Jun (and in pc-Jun) was observed in C16-treated, cholesterol-depleted cells. Of note, a similar pattern (abrogation of increase following C16 treatment) was observed with tJNK. This prevented the accumulation of tSmad2/3 and the ensuing increase in TGF-β–induced pSmad2/3 (Figure 9, A–C). These phenomena are reflected in the ability of cholesterol depletion to enhance TGF-β stimulation of Smad2/3-dependent transcription, which was concomitantly disrupted by C16 (Figure 9, D and E). We
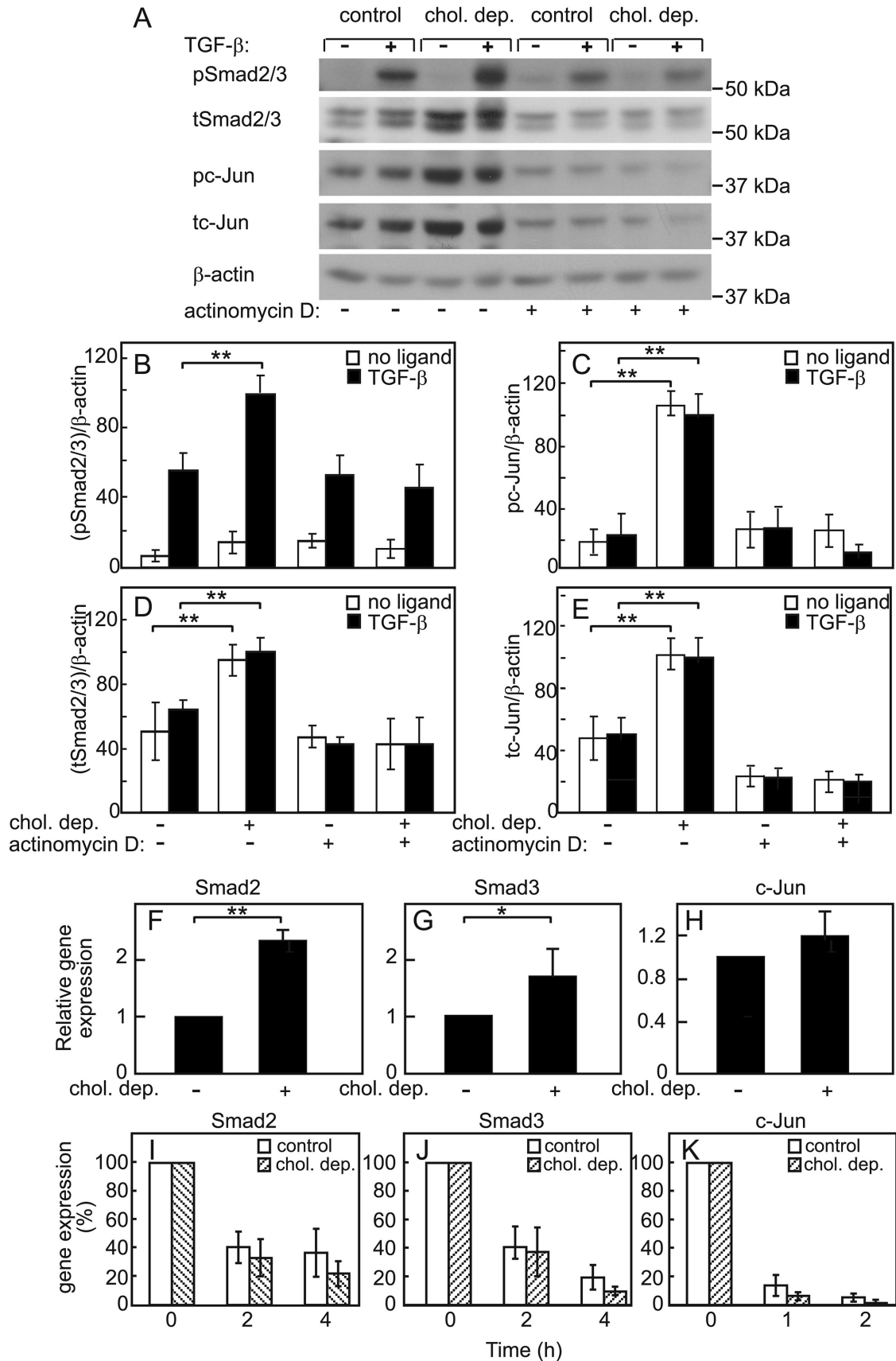
FIGURE 4: Effects of cholesterol depletion on TGF-β–mediated changes of expression of EMT markers and wound healing. (A) A representative blot of the phenotypic markers E-cadherin and Snail. The increase in the levels of tSmad2/3 and tc-Jun following cholesterol depletion is shown as control for the effectiveness of the treatment. β-Actin served as a loading control. Mv1Lu cells were subjected to statin-mediated cholesterol depletion (16 h; *Materials and Methods*), adding TGF-β1 (50 pM) for the last 12 h. The cells were then lysed and subjected to immunoblotting of E-cadherin, Snail, Smad, or c-Jun. (B, C) Quantification of E-cadherin (B) or Snail (C) levels. The untreated control sample without ligand was taken as 100%. Bars are the mean ± SEM of five independent experiments (*, $P < 0.05$; **, $P < 0.01$; Student's two-tailed *t* test). Cholesterol depletion induced a significant increase in the level of E-cadherin in the absence of hormone; however, this level was robustly reduced in the presence of TGF-β1. Expression of Snail was unaffected by cholesterol depletion, and its level was markedly enhanced by TGF-β in cholesterol-depleted cells. (D–F) Mv1Lu cells grown in 96-well plates were subjected (or not; control) to cholesterol depletion as in Figure 1. At time 0 (right after scratch), fresh medium (with serum or with LPDS for untreated and treated cells, respectively) with or without 50 pM TGF-β1 was added. The cells were monitored during wound closure using IncuCyte, and the relative wound density (% closure) in each well was determined. (D) Typical fields. Bar, 300 µm. (E) Quantification of wound closure. Data are mean ± SEM of five independent experiments (each with at least three technical repetitions) of the % of wound closure after 24 h. TGF-β enhanced cell migration and wound healing, while cholesterol depletion inhibited it. However, when the two were combined, the cholesterol-dependent inhibition disappeared. (F) Relative contribution of TGF-β to wound closure. In this representation unstimulated cells under each condition are taken as 100%. The enhancement in wound closure by TGF-β was higher following cholesterol depletion. Asterisks depict significant differences between the pairs marked by the brackets (*, $P < 0.05$; **, $P < 0.01$; Student's *t* test).

conclude that cholesterol depletion initially activates PKR, resulting in eIF2α phosphorylation, increased translation of c-Jun, and elevated expression of Smad2/3. This in turn allows for enhanced levels of pSmad2/3 in response to TGF-β stimulation, and for the ensuing transcriptional activation of TGF-β–responsive genes, mediated by pSmad3.

DISCUSSION

TGF-β signaling plays critical roles in numerous biological functions and in multiple diseases, including cancer (Markowitz *et al.*, 1995; Sanjabi *et al.*, 2009; Gatza *et al.*, 2010; Heldin *et al.*, 2012; Massague, 2012; Tan *et al.*, 2012; Meng *et al.*, 2016). Cholesterol metabolism and homeostasis are important effectors of cellular and biological

FIGURE 5: The effects of cholesterol depletion on Smad2/3, but not on c-Jun, depend on transcription. (A–E) Mv1Lu cells in six-well plates were subjected to cholesterol depletion as in Figure 1, with or without actinomycin D (1 µg/ml). After 16 h, cells were serum-starved (2 h), stimulated (or not) with TGF-β1 (50 pM, 30 min), lysed, and subjected to
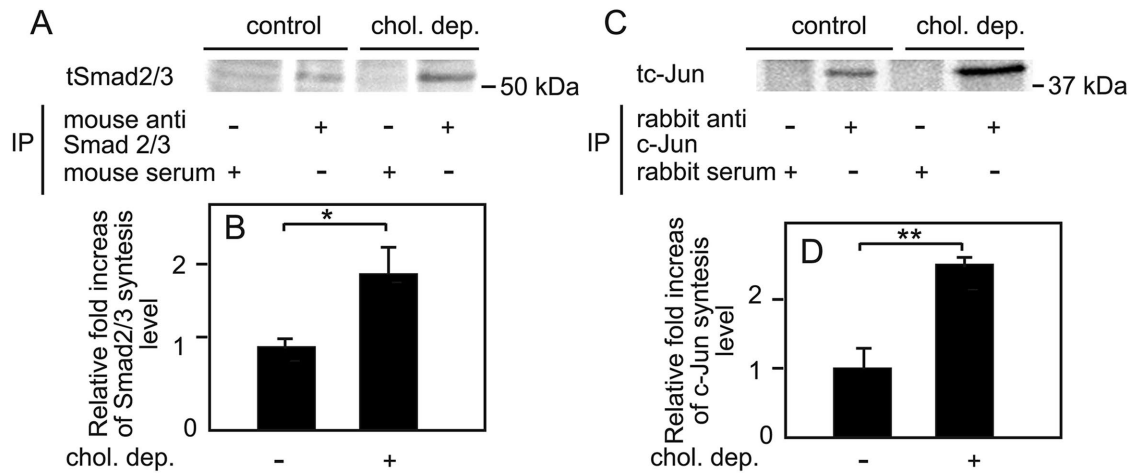
FIGURE 6: Cholesterol depletion elevates the protein synthesis (translation) of Smad2/3 and c-Jun. Mv1Lu cells in 10-cm plates were subjected (or not) to cholesterol depletion as in Figure 1. Cells were washed, starved in methionine and cystein-free medium (30 min), and labeled (25 min) with [S^{35}](Met + Cys) (*Materials and Methods*). After lysis, Smad2/3 or c-Jun was immunoprecipitated, run on SDS–PAGE, and autoradiographed. (A, C) Representative experiments. (B, D) Quantification. Band intensities were calibrated relative to the respective control, taken as 1. Bars, mean ± SEM ($n = 5$). Asterisks indicate significant increases (*, $P < 0.05$; **, $P < 0.01$) following cholesterol depletion in Smad2/3 and c-Jun translation levels.

functions in health and disease (Lim, 2011; Platt *et al.*, 2014; Mollinedo and Gajate, 2015; Zimmer *et al.*, 2016), and a high percentage of the population, especially at ages of 40 and above, are chronically treated with cholesterol-reducing drugs. While alterations in the membrane cholesterol content can alter membrane receptor interactions and signaling (Becher and McIlhinney, 2005; Kusumi *et al.*, 2005; Mollinedo and Gajate, 2015; Budi *et al.*, 2017), the effects of reduced cholesterol levels on TGF-β downstream signaling components remained unknown. Such cross-effects between cholesterol and TGF-β signaling may have important implications for diseases where TGF-β signaling is involved. Here, we studied the modulation of these parameters in cells subjected to mild (~30%) reduction in the free (membrane-associated) cholesterol content over a period long enough to explore effects on transcription, translation, and biological responses.

Cholesterol depletion by two different and independent methods (statin-mediated inhibition of cholesterol synthesis, and cholesterol absorption by HPβCD) increased constitutively the expression of mediator proteins of both canonical (Smad2/3) and noncanonical (JNK/c-Jun) TGF-β–signaling pathways (Figures 1 and 2). From this it can be concluded that the effects measured are due to reduced cholesterol

and not due to potential off-target effects of the statin. Importantly, the ratio between TGF-β–induced phosphorylated Smad2/3 and total Smad2/3 was not altered by cholesterol depletion (Figure 1 and Supplemental Figure S2), suggesting that the enhanced phosphorylation of Smad2 and Smad3 is not due to changes in the activity of the receptors, but rather reflects the higher level of tSmad2/3 present under these conditions. Thus, we propose that biological processes that affect tSmad2/3 abundance may result in differential intensity of Smad-mediated transcriptional responses, even under conditions where ligand concentration or receptor activity are similar.

To have biological significance, the above effects of cholesterol depletion should be reflected in resultant biological outcomes. In this context, it appears that at least in the Mv1Lu cell system, the downstream transcriptional activation response is mediated via pSmad3 and not pSmad2, as suggested by the markedly enhanced transcriptional activation in Smad3 but not Smad2 luciferase reporter constructs (Figure 3). TGF-β–induced transcriptional programs result in changes in cellular phenotype, such as EMT (Bhowmick *et al.*, 2001; Qiang and He, 2014; Moustakas and Heldin, 2016). Thus, cholesterol depletion per se enhanced E-cadherin expression, while significantly enhancing the ability of TGF-β to attenuate

---

immunoblotting. (A) A representative experiment ($n = 5$) demonstrating that actinomycin D prevents the elevation in Smad2/3 and c-Jun protein levels following cholesterol depletion. (B–E) Quantification of pSmad2/3, tSmad2/3, tc-Jun, and pc-Jun. The intensities of the bands were normalized to β-actin. Bars, mean ± SEM values. Results were scaled by taking in each blot the TGF-β–stimulated cholesterol-depleted sample as 100%. Asterisks indicate significant differences between control and cholesterol-depleted cells (**, $P < 0.01$; Student's *t* test). (F–H) Real-time RT-PCR analysis of Smad2 (F), Smad 3 (G), and c-Jun (H). The cells were treated (or not) by cholesterol depletion as in Figure 1, followed by RNA isolation and conversion to cDNA. Data were normalized to cDNA levels of GAPDH, taking the control cells value as 1 (see *Materials and Methods*). While the c-Jun mRNA levels were not significantly altered, those of Smad2 and Smad3 were elevated in cholesterol-depleted cells (mean ± SEM, $n = 5$; **, $P < 0.01$; *, $P < 0.05$). (I–K) Actinomycin D chase of mRNA levels. Cholesterol-depleted (or control) cells were treated (or not) with actinomycin D for different time periods (up to 4 h), and subjected to measurement of mRNA levels by real-time RT-PCR as above. To measure time-dependent alterations in the mRNA levels, data were normalized to cDNA levels of GAPDH. The level of each condition at time zero was taken as 100%. In all cases, cholesterol depletion did not stabilize the mRNAs of the tested proteins, inducing a slight (not significant) decrease in the mRNA levels.
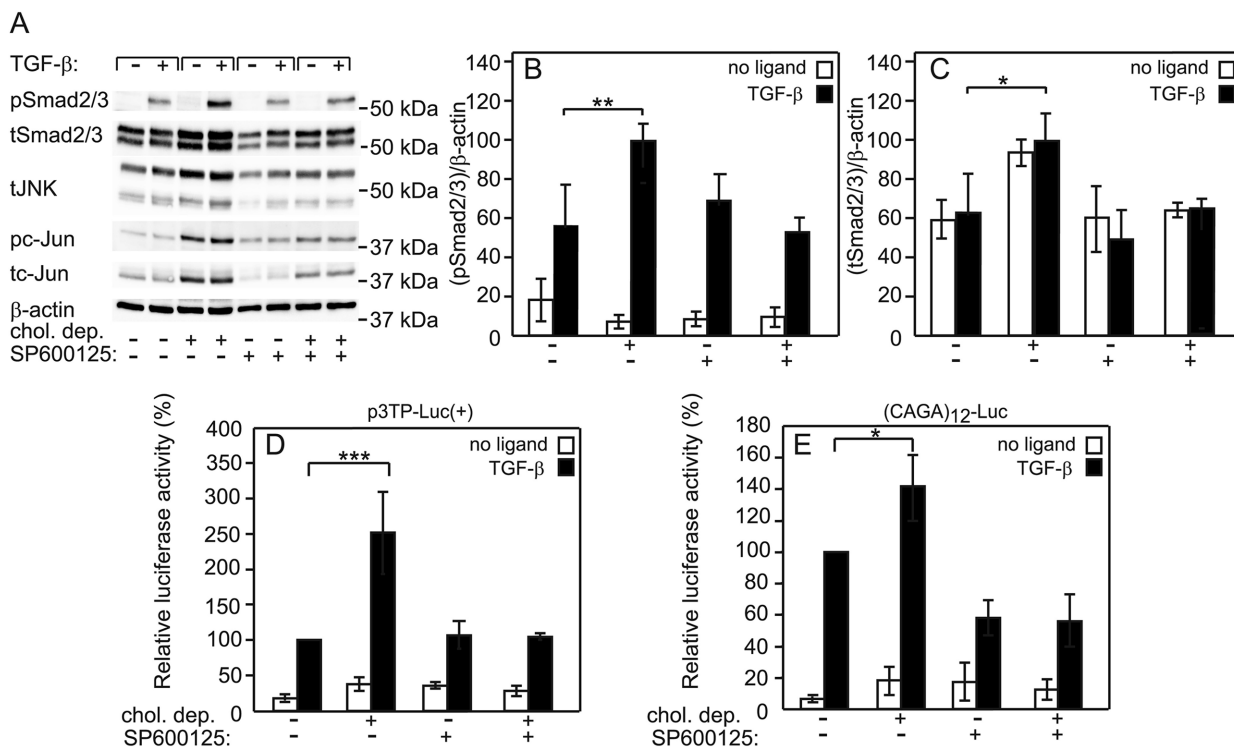
FIGURE 7: JNK activity is required for the enhancement in tSmad2/3 and pSmad2/3 by cholesterol depletion. Mv1Lu cells in six-well plates were subjected (or not) to cholesterol depletion as in Figure 1, with or without the JNK inhibitor SP600125 (added at 20 μM during the incubation period with the statin). They were then serum-starved (2 h), stimulated (or not) with TGF-β1 (50 pM, 30 min), and immunoblotted as in Figure 1. (A) A representative experiment. As expected, SP600125 inhibited the formation of pc-Jun. The cholesterol depletion-mediated elevation in tSmad2/3 and pSmad2/3 was also abrogated, indicating that the effect of cholesterol depletion on c-Jun is an upstream requirement. (B, C) Quantification of the effects on Smad2/3 (n = 5). Bands were normalized to β-actin. Bars, mean ± SEM. In each blot, the cholesterol-depleted sample stimulated with TGF-β was taken as 100%. (D, E) Quantification of the effects on Smad2/3 transcriptional activation. The experiments were conducted exactly as in Figure 3, using the TGF-β–responsive luciferase reporter plasmids p3TP-Luc(+) or (CAGA)12-Luc. At 12 h posttransfection, cells were subjected (or not; control) to statin-mediated cholesterol depletion as in Figure 1, adding SP600125 where indicated. The cells were then serum-starved, stimulated (or not) with TGF-β1, and analyzed by the DLR assay. The results were normalized for transfection efficiency using Renilla luminescence. Data are presented as the percentage of activation relative to untreated cells stimulated with TGF-β1, taken as 100%. Each bar is the mean ± SEM of five independent experiments. Asterisks indicate significant differences between control and cholesterol-depleted cells (***, $P < 0.005$; **, $P < 0.01$; *, $P < 0.05$).
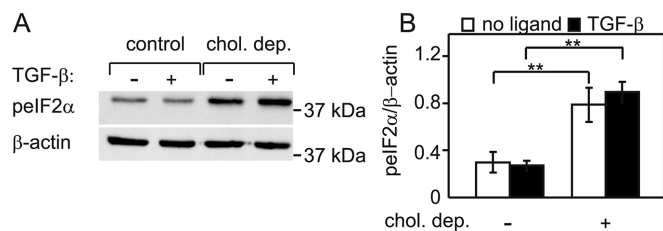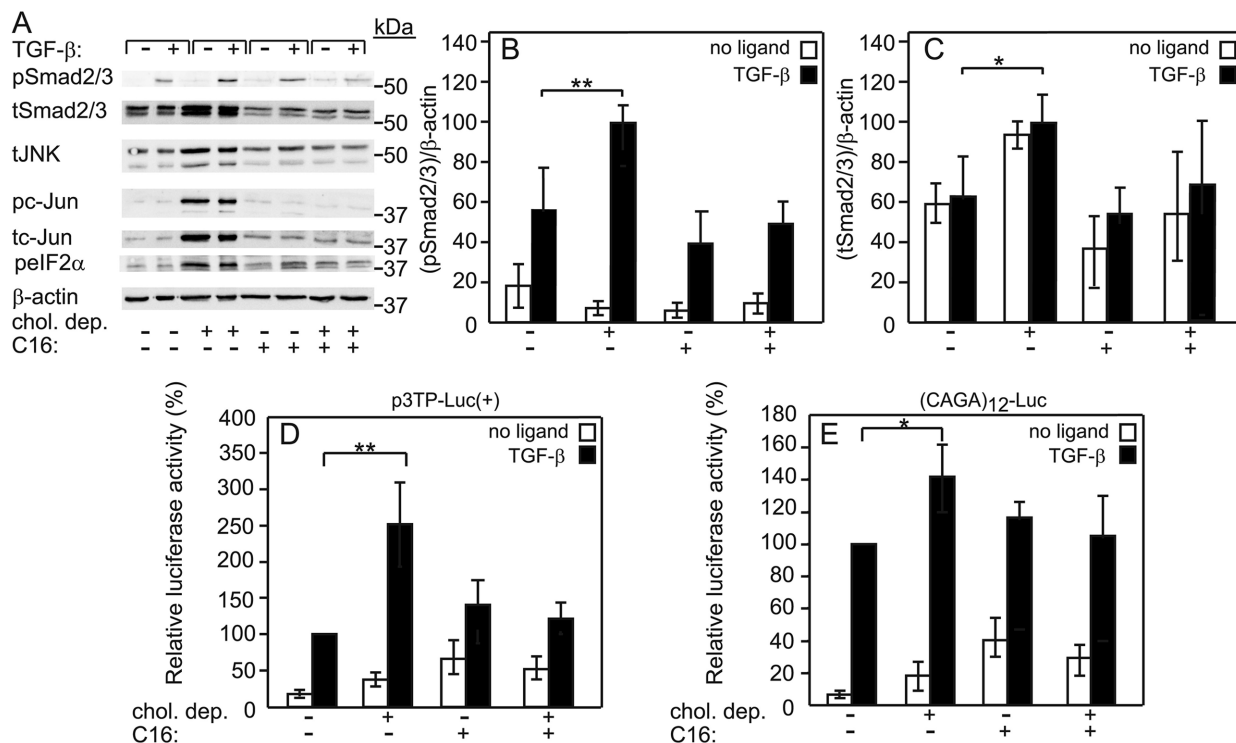

FIGURE 8: Cholesterol depletion induces eIF2α phosphorylation. Mv1Lu cells were cholesterol depleted (or not) followed by activation with TGF-β1 as in Figure 1. eIF2α phosphorylation was measured by immunoblotting for phospho-eIF2α (peIF2α). (A) A representative blot (n = 5). (B) Quantification of peIF2α levels. Bars, mean ± SEM. The cholesterol-depleted sample stimulated with TGF-β was taken as 1. Asterisks indicate significant differences between control and cholesterol-depleted cells (**, $P < 0.01$).

E-cadherin expression (Figure 4, A and B). Moreover, cholesterol depletion per se did not affect the level of Snail (an EMT-related transcription factor), and markedly enhanced its level following TGF-β stimulation (Figure 4, A and C). Both phenomena are in line

with TGF-β–induced EMT, reflecting the increased levels of phosphorylated Smad3 following ligand stimulation in cholesterol-depleted cells. These effects were mirrored by the opposing effects of cholesterol depletion per se (reduction) and TGF-β–mediated biological outcome (increase) on cell migration, measured by wound healing (Figure 4, D–F).

The ligand-independent increase in the levels of total JNK/c-Jun and Smad2/3 provides the basis for the effects of cholesterol depletion on these downstream components of TGF-β signaling pathways. Several potential mechanisms could give rise to the elevated levels of these proteins: inhibition of their degradation, increase in their translation, and/or increase in their transcription. The constitutive degradation rates of tSmad2/3 (which was very slow, in accord with the reported stability of their unphosphorylated forms; Lo and Massague, 1999; Supplemental Figure S5, A and B) and/or c-Jun (Supplemental Figure S5, C and D) were unaffected by cholesterol depletion, ruling out inhibition of degradation by reduced cholesterol as the basis for increased protein abundance. It therefore follows that the enhanced levels of Smad2/3 and c-Jun following cholesterol depletion are due to effects on their synthesis (transcription and/or translation). For Smad2/3, but not for c-Jun, cholesterol

FIGURE 9: PKR activity is required for the enhancement in tc-Jun, tSmad2/3, and pSmad2/3 by cholesterol depletion. Mv1Lu cells in six-well plates were treated (or not) to induce cholesterol depletion as in Figure 1. Where indicated, the PKR inhibitor C16 (1 µM) was added at the start of the incubation with the statin, and retained throughout the experiment. The cells were serum-starved (2 h), stimulated (or not) with TGF-β1 (50 pM, 30 min), and immunoblotted as in Figure 1. (A) A representative experiment. As expected, C16 inhibited the formation of peIF2α. The cholesterol depletion-mediated elevation in tJNK, pc-Jun, tc-Jun, tSmad2/3, and pSmad2/3 (the latter upon stimulation with TGF-β) was also abrogated, indicating that PKR activity is required for all these effects of cholesterol depletion. (B, C) Quantification of the experiments on Smad2/3 ($n = 5$). Bands were normalized to β-actin. Bars, mean ± SEM. In each blot, the cholesterol-depleted sample stimulated with TGF-β was taken as 100%. (D, E) Quantification of the effects on Smad2/3 transcriptional activation. The experiments were conducted as in Figure 7 (D and E), using the TGF-β–responsive luciferase reporter plasmids p3TP-Luc(+) or (CAGA)12-Luc. At 12 h posttransfection, cells were subjected (or not) to cholesterol depletion as in Figure 1, adding C16 where indicated. The cells were serum-starved, stimulated where indicated with TGF-β1, and analyzed by the DLR assay. The results were normalized for transfection efficiency using Renilla luminescence. Data are presented as the percentage of activation relative to untreated cells stimulated with TGF-β1, taken as 100%. Each bar is the mean ± SEM of five independent experiments. Asterisks indicate significant differences between control and cholesterol-depleted cells (**, $P < 0.01$; *, $P < 0.05$).

depletion led to elevation of the mRNA levels (Figure 5, F–H). The degradation of Smad2/3 mRNA (as well as c-Jun mRNA) was unaffected by cholesterol depletion (Figure 5, I–K), suggesting that the increase in Smad2/3 mRNA is due to their enhanced transcription and not due to inhibition of mRNA turnover. Of note, the enhanced Smad2/3 transcription resulted in a parallel and proportional increase in translation (Figure 6, A and B), indicating that the latter is a reflection of the higher mRNA transcript levels. For c-Jun, where there was no effect of cholesterol depletion on transcription, the elevated protein levels are due to enhanced translation (Figure 6, C and D).

Because both c-Jun and Smad2/3 levels are affected by cholesterol depletion, and both are transcription factors, we examined the potential interdependence of the regulation of their expression. The JNK inhibitor SP600125 abrogated c-Jun phosphorylation, and the cholesterol depletion-mediated increases in both c-Jun and Smad2/3 protein levels (Figure 7, A–C). On the other hand, inhibition of Smad2/3 phosphorylation by the kinase inhibitor SB431542 (on cells subjected to cholesterol depletion) failed to affect the increases in either c-Jun or Smad2/3 levels, as well as the activation of

c-Jun (Supplemental Figure S6, A–C). These findings place the JNK-mediated activation of c-Jun, and the ensuing elevation in c-Jun level, upstream of the effects of cholesterol depletion on Smad2/3 transcription (see model in Figure 10). In line with this conclusion, Jun family members were found to bind the promoter regions of Smad3 and Smad2 (Rouillard *et al.*, 2016). Considering that c-Jun level and activation are central for the cholesterol depletion effects, and that c-Jun is regulated at the level of translation (Figure 6, C and D), we asked whether cholesterol depletion may regulate the translation of c-Jun through eIF2α. Two lines of evidence support such a connection. First, cholesterol depletion increased the phosphorylation of eIF2α, independent of TGF-β, as occurs for c-Jun expression (Figure 8, A and B). Second, the inhibitor of the eIF2α kinase PKR (C16) abrogated the cholesterol depletion-mediated increases in eIF2α phosphorylation, c-Jun expression and phosphorylation, and the expression of Smad2/3 (Figure 9, A–C). These results lead to the model depicted in Figure 10. In this model, cholesterol depletion induces an increase in PKR activity and in the phosphorylation of its substrate, eIF2α. Under these conditions, c-Jun translation is elevated, accompanied by its phosphorylation (and activation) by JNK. The
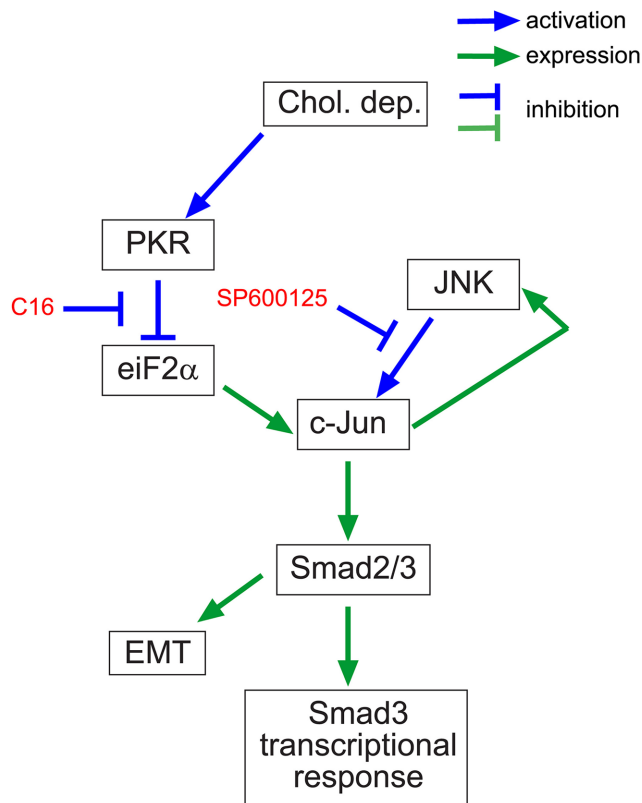
FIGURE 10: Model for regulation of c-Jun expression and Smad signaling by cholesterol depletion. Cholesterol depletion enhances Smad2/3 levels and TGF-β–induced signaling through a multistep mechanism. We propose that PKR activity is elevated following cholesterol depletion, resulting in inhibitory phosphorylation of its substrate, eIF2α, leading in turn to enhanced translation of c-Jun. The latter is phosphorylated and activated by JNK; the phosphorylated active c-Jun mediates increased expression of Smad2/3. When stimulated by hormone (TGF-β), the cholesterol-depleted cells present higher levels of pSmad2/3, due to the higher levels of tSmad2/3. In Mv1Lu cells, the end result is enhancement of Smad3-dependent transcription, and of the ensuing TGF-β–regulated biological responses (e.g., EMT).

higher level of active c-Jun results in increased expression of Smad2/3, providing the basis for the enhanced TGF-β–mediated Smad2/3 phosphorylation. Indeed, upon stimulation with TGF-β, higher levels of pSmad2/3 are formed, and the higher pSmad3 leads to enhancement of transcriptional responses, and of certain TGF-β–regulated biological phenomena. The mechanism by which cholesterol depletion activates PKR is not yet clear; PKR is regulated by multiple molecular mechanisms, including free saturated fatty acids (Nakamura et al., 2015), which may be elevated following statin treatment (Kain et al., 2015), and the involvement of these pathways is an interesting subject for further studies. It should be noted that this model is based on studies in lung epithelial cells, and it remains to be seen whether it is valid also for other cell types (e.g., cells of mesenchymal origin).

In view of the wide use of statin treatment and the well-accepted association between misregulated TGF-β signaling and multiple disease-related states (including cancer), we suggest that cholesterol depletion-mediated overactivation of TGF-β–signaling responses should be considered as a potential contributor to the side effects of statins.

MATERIALS AND METHODS

Reagents

Recombinant TGF-β1 (cat. #100-21C) was from PeproTech (Rocky Hill, NJ) and lovastatin (cat. #438185) from Merck-Calbiochem (Darmstadt, Germany). Mevalonate (as DL-mevalonic acid lactone; cat. #M4667), HPβCD (cat. #H107), protease inhibitor cocktail (cat. #P8340), phosphatase inhibitor cocktail 2 and 3 (cat. #P5726 and #P0044, respectively), and actinomycin D (cat. #A9415) were from Sigma-Aldrich (St. Louis, MO). Bovine serum albumin (BSA; fraction V) was from Roche Diagnostics (Manheim, Germany). Peroxidase-conjugated goat anti-rabbit (GαR; cat. #111-035-144) and goat anti-mouse (GαM; cat. #115-035-146) immunoglobulins G (IgGs) were from Jackson ImmunoResearch (West Grove, PA). Mouse monoclonal IgG against Smad3 reactive with Smad3 and Smad2 (cat. #sc-133098) and rabbit anti-Smad1/5/8 (cat. #sc-6031-R) were from Santa Cruz Biotechnology (Dallas, TX). Rabbit antibodies to phospho (p) Smad2/3 (cat. #8828), pSmad1/5/8 (cat. #13820), pJNK (cat. #9251), pSmad2 (cat. #3108), tSmad3 (cat. #9523), pSmad3 (cat. #9520), tJNK (cat. #9252), pc-Jun (cat. #9164), tc-Jun (cat. #9165), Snail (cat. #3879), and mouse monoclonal anti-tSmad2 (cat. #3103) were from Cell Signaling Technology (Danvers, MA). Mouse anti E-cadherin (cat. #610181) was from BD Biosciences (San Jose, CA). Rabbit anti-phospho-eIF2-α (cat. #AT-6031) was from Medical and Biological Laboratories (Nagoya, Japan). The JNK inhibitor SP600125 (competes with ATP to inhibit c-Jun phosphorylation) and the PKR inhibitor C16 were from Sigma-Aldrich. The TGF-β responsive luciferase reporter constructs p3TP-Luc(+) in pGL3 (Wrana et al., 1992; Lutz et al., 2004), (CAGA)$_{12}$-Luc in pGL3ti (Dennler et al., 1998), and pBRE-Luc were a gift from P. Knaus (Free University of Berlin, Germany). pAR3 Lux (Wrana et al., 1992) was a gift from K. Luo (University of California, Berkeley). CMV-Fast-1 wild type (wt) was a gift from B. Vogelstein (Addgene; plasmid #16521). The dual-luciferase reporter (DLR) assay system was from Promega (Madison, WI). All other reagents were from Sigma-Aldrich.

Cell culture

Mv1Lu mink lung epithelial cells (cat. #CRL-6584) from the American Type Culture Collection (Manassas, VA) were grown in DMEM as described (Ehrlich et al., 2001). MLE 12 murine lung epithelial cells (cat. #CRL-2110) were grown in DMEM:F12 (1:1) supplemented with 10% fetal calf serum (FCS). All media and cell culture reagents were from Biological Industries Beit Haemek (Beit Haemek, Israel). Cells were routinely analyzed by RT-PCR for *Mycoplasma* contamination.

Cholesterol depletion

Mv1Lu or MLE 12 cells were subjected to cholesterol depletion by statin-mediated metabolic inhibition of HMG-CoA reductase as described (Hua et al., 1996; Lin et al., 1998; Shvartsman et al., 2006). The cells were incubated (16 h) with 50 μM lovastatin and 50 μM mevalonate in medium supplemented with 10% LPDS, prepared as described earlier (Lin et al., 1998; Shvartsman et al., 2006). Mevalonate (the product of HMG-CoA reductase, added to prevent excessive reduction of mevalonate) is added at a level that reduces cholesterol production but is sufficient for farnesylation and geranylgeranylation (Shvartsman et al., 2006; Eisenberg et al., 2011). This treatment reduced the free cholesterol level, which represents almost exclusively membrane cholesterol, by 30-33% (here and in Eisenberg et al., 2006, 2013; Shvartsman et al., 2006; Supplemental Figure S1), as measured by the cholesterol assay kit (K603-100) from BioVision (Milpitas, CA) without cholesterol esterase (measuring free cholesterol).

We have shown previously that this treatment has no detectable effect on cellular phospholipids (measured by the levels of phosphatidylcholine and four different sphingomyelins) or fatty acid composition (Shvartsman et al., 2006). The general biophysical properties of the plasma membrane are also retained, as shown by the lack of effect on the lateral diffusion of nonraft membrane proteins, including K-Ras (Eisenberg et al., 2006; Shvartsman et al., 2006).

In some experiments, cholesterol extraction by HPβCD was used as an alternative to reduce membrane cholesterol. HPβCD treatment was conducted as described earlier for methyl-β-cyclodextrin (Scheiffele et al., 1997). Briefly, the medium was replaced by DMEM containing 10% LPDS, and 15 mM HPβCD were added. The cells were incubated for 16 h at 37°C, as was done for the statin treatment. The reduction in free cholesterol was similar to that in the statin-treated cells.

Immunoblotting
Mv1Lu cells were cultured overnight in six-well plates, and subjected (or not; control) to cholesterol depletion treatment. After 16 h, cells were starved in serum-free medium (2 h, 37°C), and stimulated (or not) with 50 or 100 pM TGF-β1 (30 min), followed by lysis on ice (30 min) with lysis buffer (420 mM NaCl, 50 mM HEPES, 5 mM EDTA, 1% NP-40, 3 mM dithiothreitol [DTT], protease inhibitor cocktail [#P8340; Sigma-Aldrich], and 0.1 mM Na_3VO_4). After low-speed centrifugation to remove nuclei and cell debris, the lysates were subjected to SDS–PAGE (10% polyacrylamide) and immunoblotting as described previously (Kfir et al., 2005). The blots were probed (12 h, 4°C) by primary antibodies followed by peroxidase-coupled GαR or GαM IgG (1:5000 for 1 h at 22°C). The bands were visualized by enhanced chemiluminescence (ECL) using Clarity ECL substrate (cat. #1705060; Bio-Rad, Hercules, CA), recorded using ChemiDoc Touch imaging system (Bio-Rad) and quantified by Image Lab software (Bio-Rad).

Transcriptional activation assays
Mv1Lu cells grown in 96 wells were cotransfected with Lipofectamin 2000 (Invitrogen; Thermo Fisher Scientific, Carlsbad, CA) with 1) 100 ng luciferase reporter construct, p3TP-Luc(+), (CAGA)$_{12}$-Luc, pAR3-Lux (in combination with CMV-Fast-1), and pBRE-Luc; and 2) 50 ng pRL-TK (Renilla luciferase; Promega). After 12 h, the cells were subjected to cholesterol depletion (16 h) as described above or left untreated (control). They were then serum-starved (2 h), and stimulated (or not) with 100 pM TGF-β1 (6 h for all constructs, 12 h for pAR3-Lux) in serum-free starvation medium supplemented with lovastatin and mevalonate for the cholesterol-depleted samples, and starvation medium for the control. The cells were lysed, and analyzed by the DLR assay system. The results were normalized for transfection efficiency using the Renilla luminescence.

Protein synthesis assay
Mv1Lu cells grown in 10-cm dishes were treated (or not; control) for cholesterol depletion. They were washed twice, incubated (30 min, 37°C) in L-methionine– and L-cystine–free DMEM with or without lovastatin + mevalonate, and labeled for 30 min with ^{35}S-(Met+Cys) (70 µCi/well). Cells were washed, lysed on ice (45 min) with immunoprecipitation buffer (420 mM NaCl, 50 mM HEPES, 5 mM EDTA, 1% Igepal CA-630, 3 mM DTT, protease inhibitor cocktail [1:100], phosphatase inhibitor cocktails 2 and 3 [1:100 each]). After low-speed centrifugation to remove nuclei and cell debris, lysates (1 mg protein/sample) were immunoprecipitated with 3 µg of mouse anti-Smad2/3 or rabbit anti-c-Jun antibodies for 16 h at 4°C. Protein G-Sepharose (cat. #P3296) or protein A-Sepharose 4B beads (cat. #P9424; Sigma-

Aldrich) were blocked in phosphate-buffered saline containing 3% (BSA for 16 h at 4°C, and beads (100 µl) were added to the cell lysates for 2 h at 4°C. The complexes were washed three times in immunoprecipitation buffer; bound material was solubilized in 60 µl of SDS sample buffer, subjected to SDS–PAGE (10% polyacrylamide), electrotransferred onto nitrocellulose, and subjected to autoradiography (Fluoro Image Analyzer FLA-5000; Fuji Photo Film, Tokyo, Japan).

Degradation measurements by CHX chase
Mv1Lu cells growing in six-well plates were subjected (or not; control) to the cholesterol depletion treatment (16 h). The cells were then serum-starved (2 h), incubated with 300 µM CHX for 0–6 h at 37°C, lysed, and subjected to SDS–PAGE and immunoblotting.

Real-time reverse transcriptase-PCR
Mv1Lu cells grown in six-well plates were subjected to cholesterol depletion or left untreated (control). Total RNA was isolated by EZ-RNA (cat. #20-400-100; Biological Industries, Beit HaEmek, Israel), followed by reverse transcription using a Verso RT-PCR Kit (cat. #AB-1453-B; Thermo Fisher Scientific). Real-time RT-PCR analysis of the mRNA levels of endogenous Smad2, Smad3, or c-Jun was done in triplicate using a KAPA SYBR FAST ABI Prism qPCR kit (cat. #KK-KK4604; Kapa Biosystems-Roche, Wilmington, MA), and quantified with Applied Biosystems 7300 Real-Time PCR System Software (Thermo Fisher Scientific). Gene expression values were calculated based on the comparative threshold cycle (C_T) method (Livak and Schmittgen, 2001). The real-time RT-PCR primers used were as follows: 1) For Smad2, 5′-CCCAGCA-GGAATTGAGCCAC-3′ (forward) and 5′-GAGCCTGTGTCCATACTTTG-3′ (reverse). 2) For Smad3, 5′-GGCTTTGAGGCTGTCTACCAG-3′ (forward) and 5′-CATCTGGG-TGAGGAC-CTTGT-3′ (reverse). 3) For c-Jun, 5′-GGGTGCCAAC-TCATGCTAACG-3′ (forward) and 5′-GGTCCATGCAGTTCTTG-GTC-3′ (reverse). Nontemplate controls and quantitative standards (GAPDH and β-actin) were included for calibration. For GAPDH, the primers used were 5′-CGGAGTCAACGGATTTGGTC-3′ (forward) and 5′-GAATTTGCCATGGGTGGAAT-3′ (reverse), and for β-actin, 5′-GCCATGGATGACGATATCGC-3′ (forward) and 5′-CATTCCAC-CATCACACCCT-3′ (reverse).

Wound healing cell migration assay
Mv1Lu cells were seeded (2 × 10^4 cells/well) in 96-well plates and treated (or left untreated) for cholesterol depletion (16 h). The plates were scratched with a 96-pin WoundMaker, and the medium was replaced by fresh medium fitted to the experimental condition (full medium with 10% FCS without or with 50 pM TGF-β1, or cholesterol depletion medium without or with TGF-β1). The plates were placed in the IncuCyte system (Essen Instruments, Ann Arbor, MI), which allows an automated monitoring of live cells in culture. Scratch wound closure was monitored by scanning the plates at 1 h intervals for 24 h. Images were analyzed by IncuCyte ZOOM 2016B, and the relative wound density (% closure) in each well was determined.

REFERENCES

Amsalem AR, Marom B, Shapira KE, Hirschhorn T, Preisler L, Paarmann P, Knaus P, Henis YI, Ehrlich M (2016). Differential regulation of translation and endocytosis of alternatively spliced forms of the type II bone morphogenetic protein (BMP) receptor. Mol Biol Cell 27, 716–730.

Angel P, Hattori K, Smeal T, Karin M (1988). The jun proto-oncogene is positively autoregulated by its product, Jun/AP-1. Cell 55, 875–885.

Bakin AV, Tomlinson AK, Bhowmick NA, Moses HL, Arteaga CL (2000). Phosphatidylinositol 3-kinase function is required for transforming growth factor β-mediated epithelial to mesenchymal transition and cell migration. J Biol Chem 275, 36803–36810.

Becher A, McIlhinney RA (2005). Consequences of lipid raft association on G-protein-coupled receptor function. Biochem Soc Symp 72, 151–164.

Bhowmick NA, Ghiassi M, Bakin A, Aakre M, Lundquist CA, Engel ME, Arteaga CL, Moses HL (2001). Transforming growth factor-β1 mediates epithelial to mesenchymal transdifferentiation through a RhoA-dependent mechanism. Mol Biol Cell 12, 27–36.

Budi EH, Duan D, Derynck R (2017). Transforming growth factor-β receptors and Smads: Regulatory complexity and functional versatility. Trends Cell Biol 27, 658–672.

Budi EH, Muthusamy BP, Derynck R (2015). The insulin response integrates increased TGF-β signaling through Akt-induced enhancement of cell surface delivery of TGF-β receptors. Sci Signal 8, ra96.

Chen CL, Hou WH, Liu IH, Hsiao G, Huang SS, Huang JS (2009). Inhibitors of clathrin-dependent endocytosis enhance TGFβ signaling and responses. J Cell Sci 122, 1863–1871.

Christian AE, Haynes MP, Phillips MC, Rothblat GH (1997). Use of cyclodextrins for manipulating cellular cholesterol content. J Lipid Res 38, 2264–2272.

Dennler S, Itoh S, Vivien D, ten Dijke P, Huet S, Gauthier JM (1998). Direct binding of Smad3 and Smad4 to critical TGF β-inducible elements in the promoter of human plasminogen activator inhibitor-type 1 gene. EMBO J 17, 3091–3100.

Di Guglielmo GM, Le Roy C, Goodfellow AF, Wrana JL (2003). Distinct endocytic pathways regulate TGF-β receptor signalling and turnover. Nat Cell Biol 5, 410–421.

Ehrlich M, Gutman O, Knaus P, Henis YI (2012). Oligomeric interactions of TGF-β and BMP receptors. FEBS Lett 586, 1885–1896.

Ehrlich M, Shmuely A, Henis YI (2001). A single internalization signal from the di-leucine family is critical for constitutive endocytosis of the type II TGF-β receptor. J Cell Sci 114, 1777–1786.

Eisenberg S, Beckett AJ, Prior IA, Dekker FJ, Hedberg C, Waldmann H, Ehrlich M, Henis YI (2011). Raft protein clustering alters N-Ras membrane interactions and activation pattern. Mol Cell Biol 31, 3938–3952.

Eisenberg S, Laude AJ, Beckett AJ, Mageean CJ, Aran V, Hernandez-Valladares M, Henis YI, Prior IA (2013). The role of palmitoylation in regulating Ras localization and function. Biochem Soc Trans 41, 79–83.

Eisenberg S, Shvartsman DE, Ehrlich M, Henis YI (2006). Clustering of raft-associated proteins in the external membrane leaflet modulates internal leaflet H-Ras diffusion and signaling. Mol Cell Biol 26, 7190–7200.

Gabitova L, Gorin A, Astsaturov I (2014). Molecular pathways: sterols and receptor signaling in cancer. Clin Cancer Res 20, 28–34.

Galliher AJ, Schiemann WP (2007). Src phosphorylates Tyr[284] in TGF-β type II receptor and regulates TGF-β stimulation of p38 MAPK during breast cancer cell proliferation and invasion. Cancer Res 67, 3752–3758.

Gatza CE, Oh SY, Blobe GC (2010). Roles for the type III TGF-β receptor in human cancer. Cell Signal 22, 1163–1174.

Goedeke L, Fernandez-Hernando C (2012). Regulation of cholesterol homeostasis. Cell Mol Life Sci 69, 915–930.

Gordon KJ, Blobe GC (2008). Role of transforming growth factor-β superfamily signaling pathways in human disease. Biochim Biophys Acta 1782, 197–228.

Gorin A, Gabitova L, Astsaturov I (2012). Regulation of cholesterol biosynthesis and cancer signaling. Curr Opin Pharmacol 12, 710–716.

Hanafusa H, Ninomiya-Tsuji J, Masuyama N, Nishita M, Fujisawa J, Shibuya H, Matsumoto K, Nishida E (1999). Involvement of the p38 mitogen-activated protein kinase pathway in transforming growth factor-β-induced gene expression. J Biol Chem 274, 27161–27167.

Hancock JF (2006). Lipid rafts: contentious only from simplistic standpoints. Nat Rev Mol Cell Biol 7, 456–462.

Hayashi H, Abdollah S, Qiu Y, Cai J, Xu YY, Grinnell BW, Richardson MA, Topper JN, Gimbrone MA Jr, Wrana JL, Falb D (1997). The MAD-related protein Smad7 associates with the TGFβ receptor and functions as an antagonist of TGFβ signaling. Cell 89, 1165–1173.

Heldin CH, Moustakas A (2016). Signaling receptors for TGF-β family members. Cold Spring Harb Perspect Biol 8, a022053.

Heldin CH, Vanlandewijck M, Moustakas A (2012). Regulation of EMT by TGFβ in cancer. FEBS Lett 586, 1959–1970.

Hill CS (2009). Nucleocytoplasmic shuttling of Smad proteins. Cell Res 19, 36–46.

Hocevar BA, Brown TL, Howe PH (1999). TGF-β induces fibronectin synthesis through a c-Jun N-terminal kinase-dependent, Smad4-independent pathway. EMBO J 18, 1345–1356.

Hua X, Sakai J, Brown MS, Goldstein JL (1996). Regulated cleavage of sterol regulatory element binding proteins requires sequences on both sides of the endoplasmic reticulum membrane. J Biol Chem 271, 10379–10384.

Jacobson K, Mouritsen OG, Anderson RG (2007). Lipid rafts: at a crossroad between cell biology and physics. Nat Cell Biol 9, 7–14.

Kain V, Kapadia B, Misra P, Saxena U (2015). Simvastatin may induce insulin resistance through a novel fatty acid mediated cholesterol independent mechanism. Sci Rep 5, 13823.

Kfir S, Ehrlich M, Goldshmid A, Liu X, Kloog Y, Henis YI (2005). Pathway- and expression level-dependent effects of oncogenic N-Ras: p27[Kip1] mislocalization by the Ral-GEF pathway and Erk-mediated interference with Smad signaling. Mol Cell Biol 25, 8239–8250.

Korchynskyi O, ten Dijke P (2002). Identification and functional characterization of distinct critically important bone morphogenetic protein-specific response elements in the Id1 promoter. J Biol Chem 277, 4883–4891.

Kusumi A, Ike H, Nakada C, Murase K, Fujiwara T (2005). Single-molecule tracking of membrane molecules: plasma membrane compartmentalization and dynamic assembly of raft-philic signaling molecules. Semin Immunol 17, 3–21.

Laiho M, Weis MB, Massague J (1990). Concomitant loss of transforming growth factor (TGF)-β receptor types I and II in TGF-β-resistant cell mutants implicates both receptor types in signal transduction. J Biol Chem 265, 18518–18524.

Liberati NT, Datto MB, Frederick JP, Shen X, Wong C, Rougier-Chapman EM, Wang XF (1999). Smads bind directly to the Jun family of AP-1 transcription factors. Proc Natl Acad Sci USA 96, 4844–4849.

Lim GB (2011). Vascular disease: lowering LDL cholesterol reduces atherosclerotic risk in patients with chronic kidney disease. Nat Rev Cardiol 8, 424.

Lin S, Naim HY, Rodriguez AC, Roth MG (1998). Mutations in the middle of the transmembrane domain reverse the polarity of transport of the influenza virus hemagglutinin in MDCK epithelial cells. J Cell Biol 142, 51–57.

Livak KJ, Schmittgen TD (2001). Analysis of relative gene expression data using real-time quantitative PCR and the $2^{-\Delta\Delta CT}$ method. Methods 25, 402–408.

Lo RS, Massague J (1999). Ubiquitin-dependent degradation of TGF-β-activated smad2. Nat Cell Biol 1, 472–478.

Lu Z, Murray JT, Luo W, Li H, Wu X, Xu H, Backer JM, Chen YG (2002). Transforming growth factor β activates Smad2 in the absence of receptor endocytosis. J Biol Chem 277, 29363–29368.

Lutz M, Krieglstein K, Schmitt S, ten Dijke P, Sebald W, Wizenmann A, Knaus P (2004). Nerve growth factor mediates activation of the Smad pathway in PC12 cells. Eur J Biochem 271, 920–931.

Luu W, Sharpe LJ, Gelissen IC, Brown AJ (2013). The role of signalling in cellular cholesterol homeostasis. IUBMB Life 65, 675–684.

Markowitz S, Wang J, Myeroff L, Parsons R, Sun L, Lutterbaugh J, Fan RS, Zborowska E, Kinzler KW, Vogelstein B, et al. (1995). Inactivation of the type II TGF-β receptor in colon cancer cells with microsatellite instability. Science 268, 1336–1338.

Massague J (2012). TGFβ signalling in context. Nat Rev Mol Cell Biol 13, 616–630.

Massague J, Wotton D (2000). Transcriptional control by the TGF-β/Smad signaling system. EMBO J 19, 1745–1754.

Meng XM, Nikolic-Paterson DJ, Lan HY (2016). TGF-β: the master regulator of fibrosis. Nat Rev Nephrol 12, 325–338.

Mollinedo F, Gajate C (2015). Lipid rafts as major platforms for signaling regulation in cancer. Adv Biol Regul 57, 130–146.

Motoshima H, Goldstein BJ, Igata M, Araki E (2006). AMPK and cell proliferation—AMPK as a therapeutic target for atherosclerosis and cancer. J Physiol 574, 63–71.

Moustakas A, Heldin CH (2009). The regulation of TGFβ signal transduction. Development 136, 3699–3714.

Moustakas A, Heldin CH (2016). Mechanisms of TGFβ-induced epithelial-mesenchymal transition. J Clin Med 5, 63.

Muthusamy BP, Budi EH, Katsuno Y, Lee MK, Smith SM, Mirza AM, Akhurst RJ, Derynck R (2015). ShcA protects against epithelial-mesenchymal transition through compartmentalized inhibition of TGF-β-induced Smad activation. PLoS Biol 13, e1002325.

Nakamura T, Kunz RC, Zhang C, Kimura T, Yuan CL, Baccaro B, Namiki Y, Gygi SP, Hotamisligil GS (2015). A critical role for PKR complexes with TRBP in immunometabolic regulation and eIF2α phosphorylation in obesity. Cell Rep 11, 295–307.

Parton RG, del Pozo MA (2013). Caveolae as plasma membrane sensors, protectors and organizers. Nat Rev Mol Cell Biol 14, 98–112.

Penheiter SG, Mitchell H, Garamszegi N, Edens M, Dore JJ Jr, Leof EB (2002). Internalization-dependent and -independent requirements for transforming growth factor β receptor signaling via the Smad pathway. Mol Cell Biol 22, 4750–4759.

Platt FM, Wassif C, Colaco A, Dardis A, Lloyd-Evans E, Bembi B, Porter FD (2014). Disorders of cholesterol metabolism and their unanticipated convergent mechanisms of disease. Annu Rev Genomics Hum Genet 15, 173–194.

Polak P, Oren A, Ben-Dror I, Steinberg D, Sapoznik S, Arditi-Duvdevany A, Vardimon L (2006). The cytoskeletal network controls c-Jun translation in a UTR-dependent manner. Oncogene 25, 665–676.

Qiang L, He YY (2014). Autophagy deficiency stabilizes TWIST1 to promote epithelial-mesenchymal transition. Autophagy 10, 1864–1865.

Razani B, Zhang XL, Bitzer M, von Gersdorff G, Bottinger EP, Lisanti MP (2001). Caveolin-1 regulates transforming growth factor (TGF)-β/SMAD signaling through an interaction with the TGF-β type I receptor. J Biol Chem 276, 6727–6738.

Roberts AB, Wakefield LM (2003). The two faces of transforming growth factor β in carcinogenesis. Proc Natl Acad Sci USA 100, 8621–8623.

Rosenbaum AI, Maxfield FR (2011). Niemann-Pick type C disease: molecular mechanisms and potential therapeutic approaches. J Neurochem 116, 789–795.

Rouillard AD, Gundersen GW, Fernandez NF, Wang Z, Monteiro CD, McDermott MG, Ma'ayan, A (2016). The harmonizome: a collection of processed datasets gathered to serve and mine knowledge about genes and proteins. Database (Oxford) 2016, baw100.

Sanjabi S, Zenewicz LA, Kamanaka M, Flavell RA (2009). Anti-inflammatory and pro-inflammatory roles of TGF-β, IL-10, and IL-22 in immunity and autoimmunity. Curr Opin Pharmacol 9, 447–453.

Scheiffele P, Roth MG, Simons K (1997). Interaction of influenza virus hemagglutinin with sphingolipid-cholesterol membrane domains via its transmembrane domain. EMBO J 16, 5501–5508.

Sehgal A, Briggs J, Rinehart-Kim J, Basso J, Bos TJ (2000). The chicken c-Jun 5′ untranslated region directs translation by internal initiation. Oncogene 19, 2836–2845.

Shapira KE, Gross A, Ehrlich M, Henis YI (2012). Coated pit-mediated endocytosis of the type I transforming growth factor-β (TGF-β) receptor depends on a di-leucine family signal and is not required for signaling. J Biol Chem 287, 26876–26889.

Shapira KE, Hirschhorn T, Barzilay L, Smorodinsky NI, Henis YI, Ehrlich M (2014). Dab2 inhibits the cholesterol-dependent activation of JNK by TGF-β. Mol Biol Cell 25, 1620–1628.

Shi Y, Massague J (2003). Mechanisms of TGF-β signaling from cell membrane to the nucleus. Cell 113, 685–700.

Shvartsman DE, Gutman O, Tietz A, Henis YI (2006). Cyclodextrins but not compactin inhibit the lateral diffusion of membrane proteins independent of cholesterol. Traffic 7, 917–926.

Simons K, Toomre D (2000). Lipid rafts and signal transduction. Nat Rev Mol Cell Biol 1, 31–39.

Sorrentino A, Thakur N, Grimsby S, Marcusson A, von Bulow V, Schuster N, Zhang S, Heldin CH, Landstrom M (2008). The type I TGF-β receptor engages TRAF6 to activate TAK1 in a receptor kinase-independent manner. Nat Cell Biol 10, 1199–1207.

Spruill LS, McDermott PJ (2009). Role of the 5′-untranslated region in regulating translational efficiency of specific mRNAs in adult cardiocytes. FASEB J 23, 2879–2887.

Tan CK, Chong HC, Tan EH, Tan NS (2012). Getting "Smad" about obesity and diabetes. Nutr Diabetes 2, e29.

Ventura JJ, Kennedy NJ, Lamb JA, Flavell RA, Davis RJ (2003). c-Jun NH(2)-terminal kinase is essential for the regulation of AP-1 by tumor necrosis factor. Mol Cell Biol 23, 2871–2882.

Werstuck GH, Lentz SR, Dayal S, Hossain GS, Sood SK, Shi YY, Zhou J, Maeda N, Krisans SK, Malinow MR, Austin RC (2001). Homocysteine-induced endoplasmic reticulum stress causes dysregulation of the cholesterol and triglyceride biosynthetic pathways. J Clin Invest 107, 1263–1273.

Wong C, Rougier-Chapman EM, Frederick JP, Datto MB, Liberati NT, Li JM, Wang XF (1999). Smad3-Smad4 and AP-1 complexes synergize in transcriptional activation of the c-Jun promoter by transforming growth factor-β. Mol Cell Biol 19, 1821–1830.

Wrana JL, Attisano L, Carcamo J, Zentella A, Doodey J, Laiho M, Wang X-F, Massague J (1992). TGFβ signals through a heteromeric protein kinase receptor complex. Cell 71, 1003–1014.

Wrighton KH, Feng XH (2008). To (TGF)β or not to (TGF)β: fine-tuning of Smad signaling via post-translational modifications. Cell Signal 20, 1579–1591.

Xu P, Liu J, Derynck R (2012). Post-translational regulation of TGF-β receptor and Smad signaling. FEBS Lett 586, 1871–1884.

Yamashita M, Fatyol K, Jin C, Wang X, Liu Z, Zhang YE (2008). TRAF6 mediates Smad-independent activation of JNK and p38 by TGF-β. Mol Cell 31, 918–924.

Zimmer S, Grebe A, Bakke SS, Bode N, Halvorsen B, Ulas T, Skjelland M, De Nardo D, Labzin LI, Kerksiek A, et al. (2016). Cyclodextrin promotes atherosclerosis regression via macrophage reprogramming. Sci Transl Med 8, 333ra350.

Zuo W, Chen YG (2009). Specific activation of mitogen-activated protein kinase by transforming growth factor-β receptors in lipid rafts is required for epithelial cell plasticity. Mol Biol Cell 20, 1020–1029.